Graphene on amorphous HfO_2 surface: An *ab initio* investigation

W. L. Scopel*
Departamento de Ciências Exatas, Universidade Federal Fluminense, 277255-250 Volta Redonda, RJ, Brazil and Departamento de Física, Universidade Federal do Espírito Santo, Vitória 299075-910, ES, Brazil

A. Fazzio
Instituto de Física, Universidade de São Paulo, São Paulo, and C.P. 66318, 05315-970 São Paulo, SP, Brazil

R. H. Miwa† and T. M. Schmidt
Instituto de Física, Universidade Federal de Uberlândia, C.P. 593, 38400-902 Uberlândia, MG, Brazil
(Received 16 January 2013; published 25 April 2013)

The energetic stability, electronic, and structural properties of graphene adsorbed on the amorphous HfO_2 surface (G/HfO_2) have been examined through *ab initio* theoretical investigations. We have considered the graphene adsorption on (i) defect-free (pristine) and defective HfO_2 surfaces, (ii) oxygen vacancy, and (iii) interstitial oxygen atoms. We find that the formation of G/HfO_2 is an exothermic process, ruled by van der Waals interactions. In (i) and (iii) there is no net charge transfer between the graphene and the HfO_2 surface. In contrast, upon the presence of oxygen vacancy, the adsorbed graphene sheet becomes *n*-type doped, due to a donor level lying above the Dirac point of the graphene. The absence of G–HfO_2 chemical bonds has been maintained, however, the graphene adsorption energy increases when compared with (i) and (iii). Finally, in (ii) we find that HfO_2 surface potential becomes more inhomogeneous, strengthening the formation of electron- and hole-rich regions on the graphene sheet.

DOI: 10.1103/PhysRevB.87.165307 PACS number(s): 73.20.−r, 73.20.At, 73.22.Pr

I. INTRODUCTION

The electronic and structural properties of graphene may change upon its interaction with solid surfaces. Indeed, scanning tunneling microscopy (STM) images indicate a "spatially dependent perturbation" in graphene sheets lying on dielectric surfaces.[1] The adsorbed graphene follows the surface corrugation, giving rise to a charge density fluctuations, i.e., electron- and hole-rich regions ("electron-hole puddles"), and thus an inhomogeneous graphene surface potential.[2] Such surface potential inhomogeneity will contribute to the reduction of carrier mobility. For instance, graphene on silicon oxide surface exhibits an electronic mobility reduction of around one order of magnitude in comparison with the isolated graphene.[3,4] Moreover, the presence of impurities or intrinsic defects at the graphene–substrate (G–substrate) interface region promotes not only the reduction of the carrier mobility, but also the doping process of the graphene sheet. There are experimental results indicating an *n*- or *p*-type doping of graphene adsorbed on SiO_2 surface mediated by the presence of atmospheric oxygen,[5] or self-assembled atomic or molecular structures at the G–SiO_2 interface.[6] Very recently we have proposed an *n*-type doping of graphene ruled by the presence of threefold coordinated oxygen atoms embedded in the SiO_2 substrate.[7]

High dielectric constant (κ) materials promote a better screening of the charged impurities or intrinsic defects at graphene–dielectric interfaces.[8] This is an important property to design electronic nanodevices based on graphene, for instance, top-gated field-effect-transistors (FET) like HfO_2/graphene/SiO_2[9,10] or HfO_2/graphene/SiC.[11,12] However, there are some controversial results on the G–HfO_2 interface. For high-quality HfO_2 films deposited on graphene, recent experimental findings indicate a carrier mobility limitation to 20 000 cm^2/V s, due to the phonon scattering processes.[9] Meanwhile, lower carrier mobility (around 5000 cm^2/V s), with a weak temperature dependence, has been obtained for graphene adsorbed by thin films (up to 4 nm) of HfO_2.[13] In addition, *n*- as well as *p*-type doping of the graphene sheet have been verified, due to the presence of intrinsic defects and/or impurities at the G–HfO_2 interface.[10,11,13] Regarding the structural and the energetic properties, it has been proposed that the graphene sheet is attached to the HfO_2 surface through van der Waals (vdW) interactions, with the graphene sheet lying 5 Å from the HfO_2 surface.[10] Whereas other experimental results suggest the formation of C–O covalent bonds at the graphene–HfO_2 interface.[14]

Atomistic simulations may provide a clear understanding of the energetic, structural, and electronic properties of graphene sheets adsorbed on solid surfaces. Thus, motivated by the scenario described above, we have performed an *ab initio* theoretical investigation of G/HfO_2. In order to provide a more realistic boundary condition to the G–HfO_2 interface, we have considered an amorphous HfO_2 surface. On the pristine HfO_2 surface we obtained a G–surface equilibrium distance of 3.29 Å, and an adsorption energy of 23 $meV/Å^2$ ruled by vdW interactions. There are no chemical bonds at the interface. We find a small energy gap at the Dirac point attributed to the graphene interaction with the HfO_2 surface, however, we did not find any $G \leftrightarrow HfO_2$ net charge transfer at the G–HfO_2 interface. Upon the presence of oxygen vacancy (O_v), the adsorbed graphene sheet becomes *n*-type doped. In this case, the adsorption energy increases to $\sim$33 $meV/Å^2$, and the graphene–surface distance reduces to around 3.0 Å. In contrast, there is no such increase on the graphene adsorption energy, and electronic charge transfers, by the presence of interstitial oxygen atoms embedded in HfO_2 surface.

 ©2013 American Physical Society

II. METHODOLOGY

The amorphous structure was generated through *ab initio* molecular dynamics (MD) simulations based on the DFT approach as implemented in the VASP code.[15,16] The calculations were performed using pseudopotentials[17] and the generalized gradient approximation (GGA) for the exchange-correlation potential.[18] In Ref. 19 we present details on the generation procedure of amorphous HfO_2 bulk structure. In order to generate the amorphous HfO_2 slab we have broken the boundary condition at the z direction by introducing a vacuum at 10 Å. The lattice mismatch between the adsorbed graphene sheet, and the amorphous HfO_2 surface, can be avoided by taking a suitable choice for (slab) lattice constants of the amorphous HfO_2 surface, namely xy surface plane. In this work we have considered lattice constants of $5a$ and $3a\sqrt{3}$, along the x and y directions, respectively, where a is the calculated equilibrium lattice constant of the graphene sheet, 2.46 Å. Once we obtained a well described amorphous HfO_2 surface, we investigated the equilibrium geometry, energetic stability, and the electronic properties of a graphene sheet adsorbed on the HfO_2 surface. Herein we have turned on the van der Waals (vdW) interaction described within a semiempirical approach following the Grimme formula.[20] We used a supercell, a plane-wave-cutoff energy of 400 eV, and the Brillouin zone was sampled at the Γ point. In all calculations the lattice parameter was kept fixed at the calculated value, whereas the atoms were allowed to relax until the atomic forces were smaller than 0.025 eV/Å.

III. RESULTS AND DISCUSSIONS

A. Graphene on pristine HfO_2

In Fig. 1(a) we present the structural model of the G/HfO_2 system. At the equilibrium geometry the graphene sheet lies at 3.29 Å from the HfO_2 surface. There are no covalent bonds at the G–HfO_2 interface, which is in agreement with recent experimental findings.[10,11,14] The energetic stability of the graphene sheet adsorbed on the HfO_2 surface was examined through the calculation of the graphene adsorption energy (ΔE^{ads}),

$$\Delta E^{\text{ads}} = E[\text{G}] + E[\text{HfO}_2] - E[\text{G/HfO}_2].$$

Where E[G] and E[HfO_2] represent the total energies of the isolated components, graphene sheet, and HfO_2 surface, respectively, and E[G/HfO] is the total energy of the (final) graphene adsorbed system G/HfO_2. Here we have considered the graphene adsorption on two different HfO_2 amorphous surfaces, where we find adsorption energies of 23 meV/Å^2 (61 meV/C atom). The formation of G/HfO_2 is an exothermic process. Previous theoretical results, for graphene adsorbed on oxygen terminated cubic HfO_2(111) surface, indicate a slightly smaller G–HfO_2 equilibrium distance (3.05 Å), and the graphene adsorption energy is almost twice (110 meV/C atom) as compared with our results.[21] In this case we can infer that, although the same material (HfO_2), the atomic structure of the substrate plays an important role on the energetic stability of G/HfO_2 systems. In addition, comparing with the G/SiO_2 partner system,[1,7] we verify that the graphene sheet is more strongly attached to the HfO_2 substrate, presenting a smaller G–surface equilibrium distance. The smaller vertical distance and the higher adsorption energy of G/HfO_2, when compared with G/SiO_2, are in qualitative agreement with the recent experimental measurements.[10] Furthermore, we verified that, similar to the G/SiO_2 system, the energetic stability of G/HfO_2 is (mostly) mediated by vdW interactions. Indeed, by turning off the vdW contribution from our total energy calculations, ΔE^{ads} reduces to 3.5 meV/Å^2 (9.2 meV/C atom), and G–HfO_2 equilibrium distance increases to 4.6 Å.

There is a charge density fluctuation ($\Delta\rho$) on the adsorbed graphene upon the formation of G/HfO_2. Such a charge density fluctuation can be measured by comparing the total charge densities of the isolated components, namely graphene sheet (ρ[G]) and HfO_2 surface (ρ[HfO_2]), both keeping the same

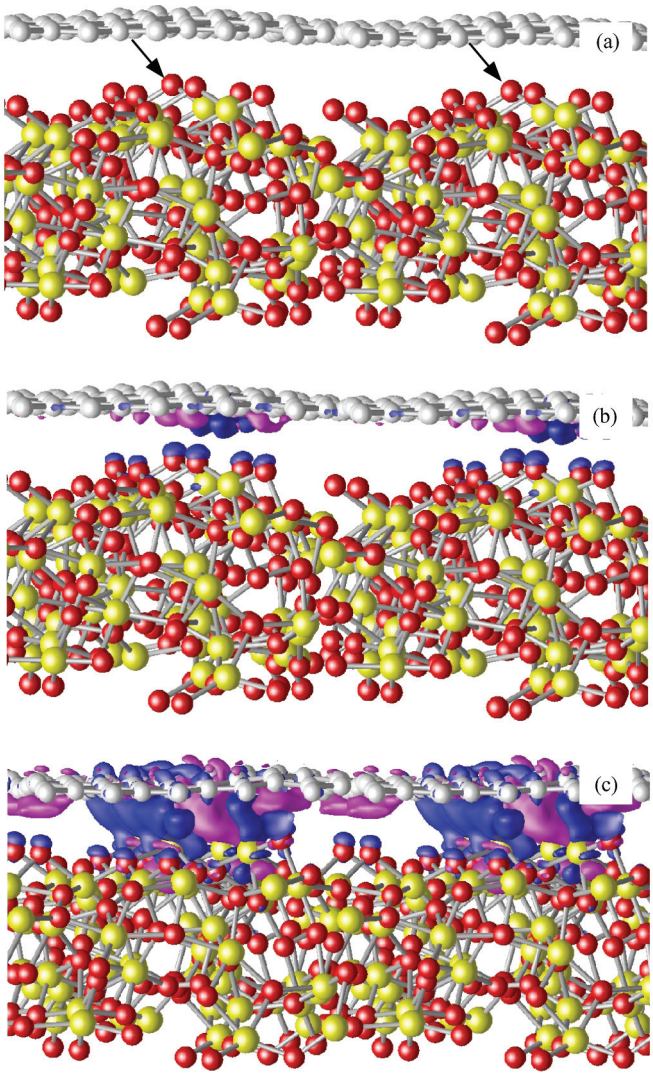

FIG. 1. (Color online) (a) The relaxed atomic structure of graphene adsorbed on the HfO_2 surface G/HfO_2. The gray, red, and yellow spheres represent the atomic species C, O, and Hf, respectively. Net charge transfers $\Delta\rho$ for the (b) defect free and (c) defective (V_O) G/HfO_2 systems. Blue regions indicate a net charge density gain ($\Delta\rho > 0$), and pink regions indicate a net charge density loss ($\Delta\rho < 0$) relative to the isolated systems. In (a) the arrows indicate the position of oxygen vacancy on the surface.

equilibrium geometry as that of G/HfO_2, and the total charge density of the (final) G/HfO_2 system (ρ[G/HfO_2]),

$$\Delta\rho = \rho[\mathrm{G/HfO_2}] - \rho[\mathrm{G}] - \rho[\mathrm{HfO_2}].$$

Figure 1(b) depicts our result of $\Delta\rho$, where the increase (decrease) on the total charge density $\Delta\rho > 0$ ($\Delta\rho < 0$) is indicated by pink (blue) regions. There are no covalent bonds attaching the graphene to the HfO_2 surface, and it is noticeable the formation of localized electron-rich as well as hole-rich regions at the G–HfO_2 interface. However, there is no net charge transfer between the adsorbed graphene and the HfO_2 substrate. Meanwhile, some recent experimental findings indicate a p-type[10,11] as well as an n-type doping of graphene adsorbed on the HfO_2 surface.[13] We believe that those graphene doping processes may occur by the presence of impurities or structural defects at the G–HfO_2 interface. For instance, oxygen vacancies, which will be discussed in the next section.

We next examined the electronic properties of G/HfO_2. Figure 2(a) presents the electronic density of states (DOS) of G/HfO_2, and the projected DOS (PDOS) of the HfO_2 surface and the adsorbed graphene sheet. We find that the HfO_2 surface exhibits an energy gap of 3.3 eV, and the Fermi level of G/HfO_2 lies at the graphene Dirac point. The PDOS presented in Fig. 2(a) are quite similar to the ones of the separated components (isolated graphene sheet and HfO_2 surface), thus indicating that the electronic structures of the graphene sheet and the HfO_2 surface are weakly perturbed due to the formation of G/HfO_2. This is in agreement with the noncovalent interaction between the graphene sheet and the HfO_2 surface. In addition, by using the procedure proposed in Ref. 22, we examine the electronic structure of the HfO_2 surface and graphene sheet before the formation of G/HfO_2. Here we have considered the energy level of an isolated hydrogen molecule (within our supercell) as a reference to line up the electronic bands of the components. We find that the Dirac point of the isolated graphene sheet lies within the band gap of the HfO_2 surface, Fig. 3(left). In this case there are not allowed empty (filled) states below (above) the Dirac point in order to promote a p-type (n-type) doping of the adsorbed graphene sheet. Those results support the absence of a net electronic charge transfer from/to the adsorbed graphene.

Upon the formation of G–HfO_2 interface, the energy bands of the graphene sheet are mostly preserved, however, there is an energy gap at the K point composed by π and π^* states. We find an energy gap of 9.1 meV, which is comparable with the ones obtained for similar graphene/oxide systems.[21,23] Here the energy gap on the graphene is ruled by (i) its structural deformation, and (ii) the electrostatic interaction between the graphene sheet and the amorphous HfO_2 surface. In (i) we calculate the electronic band structure of an isolated graphene sheet, keeping the equilibrium geometry of the G/HfO_2 system, where we find an energy gap of 6.6 meV. The graphene sheet presents a corrugation of 0.15 Å.[24] In this case we can infer that the rest (2.5 meV) is due to (ii). In order to provide further support to (ii), we have examined the energy gap of a flat graphene sheet as a function of its vertical distance with respect to the HfO_2 surface. In this case we find energy gaps of 1.6 and 8.4 meV for vertical distances of 4.14 and 3.71 Å, respectively.

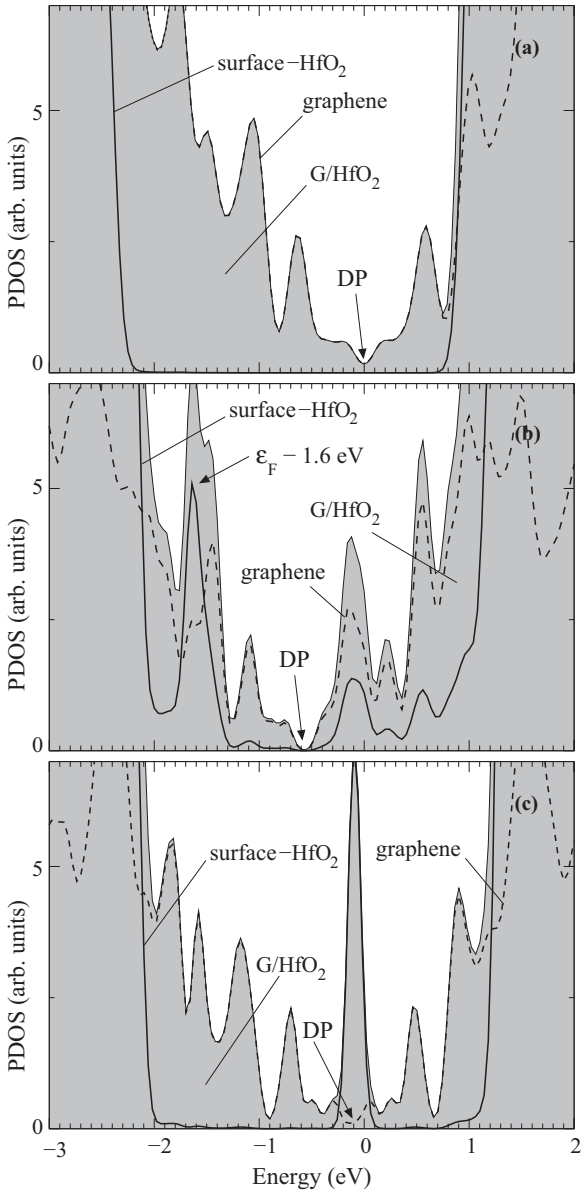

FIG. 2. Density of states of G/HfO_2. Pristine HfO_2 surface (a), and defective HfO_2 surface, with the V_O at the surface (b), and subsurface (c) sites. The Fermi level is set to zero. Shaded regions represent the total density of states (G/HfO_2), solid thick lines indicate the projected density of states on the HfO_2 surface, and the dashed lines indicate the projected density of states on the adsorbed graphene sheet.

That is, the opening of the energy gap of graphene has been strengthened upon its interaction with the HfO_2 surface.

B. Oxygen vacancy

There are several ways to get an n- or p-type doping of graphene interacting with solid surfaces. For instance, by the presence of foreign atoms or molecules at the G–surface interface,[5,6] or through the formation of intrinsic defects, like dangling bonds, in the graphene substrate.[7,25] In a recent experimental study, the n-type doping of graphene has been attributed to the formation of oxygen vacancies (V_O) in HfO_2

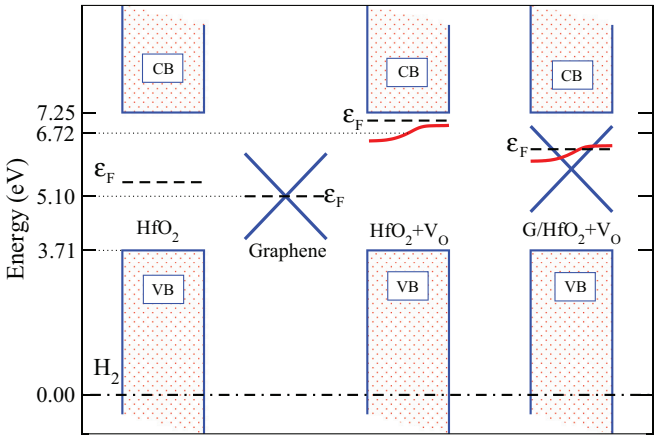

FIG. 3. (Color online) Schematic energy diagram for isolated systems, (left) HfO_2 surface, and graphene sheet, (center) defective HfO_2 surface ($HfO_2 + V_O$). (Right) Graphene adsorbed on the HfO_2 upon the presence of V_O ($G/HfO_2 + V_O$). Dashed lines represent the Fermi energy for each system calculated separately, and the the solid (red) line represent the V_O impurity level. The horizontal dot-dashed line is the energy position of the common reference for the H_2 molecule level.

films deposited on the graphene sheet.[13] Indeed, V_O has been considered as a dominant intrinsic defect in electronic (nano)devices composed by HfO_2.[26,27] The energetic stability of V_O can be examined by the calculation of its formation energy (E_f),

$$E_f = E[V_O] - n_{Hf}\mu_{Hf} - n_O\mu_O.$$

Here $E[V_O]$ is the total energy obtained from our supercell calculations, upon the presence of V_O, and n_{Hf} (n_O) indicates the number of Hf (O) atoms in the supercell. At the thermodynamic equilibrium, the Hf and O chemical potentials are constrained by $\mu_{Hf} + 2\mu_O = \mu_{[HfO_2]}$, where $\mu_{[HfO2]}$ is the total energy of HfO_2 (amorphous) bulk phase. At the oxygen-rich condition we will have $\mu_O = \mu_O^{max} = \mu_{[O_2]}$, where $\mu_{[O_2]}$ is total the energy of an oxygen atom in an isolated triplet O_2 molecule.[28]

By using the same calculation approach as presented in this work, we examined the energetic stability of V_O in amorphous HfO_2 bulk phase,[19] where we obtained E_f between 5.49 and 6.58 eV, at the oxygen-rich condition $\mu_O = \mu_O^{max}$. That is, different from the monoclinic phase, in the amorphous HfO_2 we face a large number of (possible) vacancy sites, giving rise to an energy interval of 1.09 eV to the V_O formation energy. Here, by considering a number of different sites for V_O defects in the amorphous HfO_2 surface, we find similar results for the V_O formation energy, 6.5 eV. While for a V_O lying at around 4.02 Å below the surface, we obtained E_f of 6.8 eV. It is worth noting that those results of E_f were obtained for $\mu_O = \mu_O^{max}$ (oxygen-rich limit), while at the oxygen-poor condition $\mu_O = \mu_O^{min} = \Delta H_{[HfO_2]}/2 + \mu_{[O_2]}$, the formation of V_O becomes more likely E_f = 0.73 and 1.03 eV, respectively. While at the stoichiometric condition $\mu_O = \bar{\mu}_O = (\mu^{max} + \mu^{min})/2$ we find E_f = 3.62 and 3.92 eV, respectively.[29] Here we have considered the experimental result of $\Delta H_{[HfO_2]} = 266$ cal/mol.[30] Regarding the electronic structure, for both sites, neutral V_O gives rise to a defect level localized within the HfO_2 band gap, close to the bottom of the conduction band, being occupied with two electrons (a donor level), Fig. 3(center). Similar results have been obtained for neutral V_O in HfO_2 crystalline bulk phase.[31] The presence of V_O strongly modify the G–HfO_2 interaction picture.

Figure 1(c) presents a map of the charge density fluctuation $\Delta\rho$ of the G/HfO_2 system upon the presence of V_O on the HfO_2 surface. One observes that (i) the electronic interaction at the G–HfO_2 interface has been strengthened, and (ii) the charge density inhomogeneity (electron- and hole-rich regions) on the adsorbed graphene sheet has been increased, with the formation of electron-hole puddles. (i) Can be quantified through the calculation of the graphene adsorption energy, where we find $\Delta E^{ads} = 36$ meV/Å^2 (96 meV/C atom), and the G–HfO_2 equilibrium distance reduces to 3.04 Å. The graphene adsorption energy is slightly small for V_O at the subsurface site $\Delta E^{ads} = 31.0$ meV/Å^2 (80.5 meV/C atom), with G–HfO_2 equilibrium distance of 3.00 Å. However, it is worth noting that even for the defective HfO_2 surface, the energetic stability of G/HfO_2 is ruled by vdW interactions. Here, by turning off the vdW contribution, we obtained $\Delta E^{ads} = 3.9$ meV/Å^2 (10.5 meV/C atom). Comparing with the previous results of $\Delta\rho$ for graphene on the defect-free HfO_2 surface [Fig. 1(b)] we can infer that (ii) is due the strengthening of the surface potential inhomogeneity by the presence V_O defects on the HfO_2 surface. Indeed, it is noticeable that the electronic charge transfers $\Delta\rho$ at the G–HfO_2 interface are mostly localized nearby the V_O sites. Similarly, such electron–hole puddles have been observed for graphene on the amorphous SiO_2 surface.[2,7,32]

As the impurity level is strongly localized, its position with respect to the HfO_2 valence band is weakly modified due to the adsorption of the graphene. As depicted in Fig. 3(center), for V_O lying on the HfO_2 surface, the Dirac point (of the isolated graphene sheet) lies below the occupied V_O donor level, and 0.15 eV below the Fermi level $\varepsilon_F - 0.15$ eV of the defective HfO_2 surface. Within this scenario, in order to establish the electronic equilibrium at the G–HfO_2 interface, electrons tunnel out from the HfO_2 surface into the adsorbed graphene sheet [Figs. 3(center) → 3(right)]. A similar energy level picture has been verified for V_O in the subsurface site. Indeed, the calculated DOS and PDOS of the G/HfO_2 system with V_O lying on the surface [Fig. 2(b)] and subsurface [Fig. 2(c)] sites show the Dirac point lying at $\varepsilon_F - 0.57$ and $\varepsilon_F - 0.12$ eV, respectively. That is, the presence of V_O on HfO_2 gives rise to an n-type doped graphene by the formation of G/HfO_2. However, the electronic, energetic, and structural properties of the G/HfO_2 will depend on the local equilibrium geometry around the defect site V_O, viz, (i) for V_O on the HfO_2 surface, we find additional states on the PDOS [$\varepsilon_F - 1.6$ eV in Fig. 2(b)] attributed to the hybridizations of the surface atoms around the defective site. (ii) The defect level is more localized for V_O buried below the HfO_2 surface [Fig. 2(c)], and its interaction with the graphene sheet is somewhat reduced when compared with the V_O on the surface site. Indeed, based on the Bader charge density analysis,[33] we calculate an amount of the charge transfer to the adsorbed graphene sheet of 0.008 e (0.003 e) per vacancy defect at the HfO_2 surface (subsurface) sites, which induce around 5.0×10^{11}/cm^2 (1.9×10^{11}/cm^2) carriers into graphene with zero bias voltage. Thus, we can

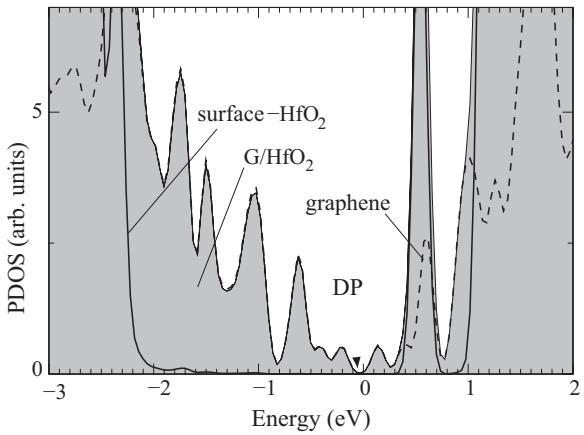

FIG. 4. Density of states of defective (O_i) HfO_2 surface. The Fermi level is set to zero. Shaded regions represent the total density of states (G/HfO_2), solid thick lines indicate the projected density of states on the HfO_2 surface, and the dashed lines indicate the projected density of states on the adsorbed graphene sheet.

infer that there is a dependence between the localization of the V_O defect site in G/HfO_2, and the net charge transfer to the adsorbed graphene sheet. At the thermodynamic equilibrium, the concentration of the V_O defects ($c[V_O]$) can be obtained by

$$c[V_O] = N_{V_O} e^{-E_f/k_B T}.$$

Here E_f is the formation energy, and N_{V_O} represents the number of lattice sites (per unit volume) where we may find the defect (oxygen vacancy), k_B is the Boltzmann's constant, and T is the temperature. In this case the carrier concentration (n) on the adsorbed graphene sheet can be estimated. At $T = 900$ K, typical G/HfO_2 annealing temperature,[11] we find a negligible electronic carrier concentration $n = 1.0 \times 10^{-16}\, e/V_O$ ($6 \times 10^{-3}\ cm^{-2}$) at the oxygen-rich limit ($\mu_O = \mu^{max} \rightarrow E_f = 6.5$ eV). However, at the stoichiometric condition ($\mu_O = \bar{\mu}_O \rightarrow E_f = 3.62$ eV) we obtain $n = 1.3\, e/V_O$ ($8 \times 10^{13}\ cm^{-2}$). If for one side the presence of charge accumulation at the G–HfO_2 interface is important as a top gate dielectric layer, the ionization of the V_O impurity (donor) level leads to a charged impurity concentration by the same order of the carriers one, resulting in a reduction of the mobility. Actually Fallahazad *et al.*[13] observed a decreasing of the carrier mobility when thin films of HfO_2 are deposited on graphene.

In addition, we have examined another intrinsic point defect in HfO_2, interstitial oxygen (O_i). Similarly to V_O, we have considered O_i, lying on the HfO_2 amorphous surface, and buried below the HfO_2 surface, where we find formation energies of 0.68 and 2.6 eV, respectively, at the oxygen-rich condition. The latter formation energy is close to one obtained by Foster *et al.*[34] for fourfold-coordinated O_i in monoclinic HfO_2. It is worth noting that by reducing the oxygen concentration ($\mu_O \rightarrow \mu_O^{min}$) the energetic cost to the formation of O_i increases. For both configurations, the formation of O_i is an endothermic process with respect to the separated components, namely, HfO_2 surface and an isolated O_2 molecule. However, there is a clear energetic preference for the formation of O_i on the surface site. This is in agreement with the formation of oxygen-rich HfO_2 amorphous surface upon the MD simulations. However, different from V_O, the graphene adsorption energy is the same compared with the pristine G/HfO_2 system. We find $\Delta E^{ads} = 24$ meV/Å^2 (64 meV/C atom). Furthermore, there is no net electronic charge transfer at the G–HfO_2 interface, namely, an n- or p-type doping of graphene upon the presence of (neutral) O_i defects in HfO_2 is not expected. The electronic density of states, presented in Fig. 4, is in agreement with the weak graphene–surface interaction, as well as the no net charge charge transfer upon the presence of O_i in the HfO_2 surface.

IV. SUMMARY

In summary, based on *ab initio* calculations, we have examined the energetic stability, electronic, and structural properties of graphene adsorbed on the amorphous HfO_2 surface. We find that there are no chemical bonds at the graphene–HfO_2 interface, where the vdW interactions rule the energetic stability of the G/HfO_2 system. In this case, the energy band dispersions of the adsorbed graphene has been preserved. However, due to the interaction with the HfO_2 surface, and its structural deformations (i.e., graphene sheet corrugation), a small energy gap takes place at the K point. The HfO_2 surface induces a charge density displacement on the adsorbed graphene, giving rise to electron- and hole-rich regions nearby the G–HfO_2 interface. There is no substantial net charge transfer between the graphene sheet and the defect-free HfO_2 surface. Whereas, upon the presence of oxygen vacancy in HfO_2, the graphene sheet becomes n-type doped. The oxygen vacancy gives rise to a donor level just below the HfO_2 conduction band, and above the Dirac point of the adsorbed graphene. In order to reach an electronic equilibrium, there is a charge transfer from the HfO_2 donor level (becoming partially occupied) to the adsorbed graphene sheet (becoming n-type doped). Regarding the energetic, and structural properties, the graphene adsorption on the HfO_2 surface is ruled by the vdW interations, where we find a graphene adsorption energy of 23 meV/Å^2 on the defect-free HfO_2 surface. Such graphene–HfO_2 interaction has been strengthened by the presence of oxygen vacancies on the HfO_2 surface, and subsurface sites ($\Delta E^{ads} = 36$, and 31 meV/Å^2, respectively). In contrast, we find that interstitial oxygen atoms do not change the graphene adsorption energy, compared with the pristine G/HfO_2 system, and there is no net electronic charge transfer at the G–HfO_2 interface.

ACKNOWLEDGMENT

The authors acknowledge financial support from the Brazilian agencies CNPq, FAPEMIG, and FAPESP and the CENAPAD-SP for computer time.

*wlscopel@gmail.com
†hiroki@infis.ufu.br

[1] M. Ishigami, J. H. Chen, W. G. Cullen, M. S. Fuhrer, and E. D. Williams, Nano Lett. **7**, 1643 (2007).

[2]J. Martin, N. Akerman, G. Ulbricht, T. Lohmann, J. H. Smet, and K. Von Klitzing, Nat. Phys. **4**, 144 (2008).
[3]M. C. Lemme, T. J. Echtermeyer, M. Bauss, and H. Kurz, IEEE Electron Device Lett. **28**, 282 (2007).
[4]V. E. Dorgan, M.-H. Bar, and E. Pop, Appl. Phys. Lett. **97**, 082112 (2010).
[5]S. Ryu, L. Liu, S. Berciaud, Y.-J. Yu, H. Liu, P. Kim, G. W. Flynn, and L. E. Brus, Nano Lett. **10**, 4944 (2010).
[6]Z. Yan, Z. Sun, W. Lu, J. Yao, U. Zhu, and J. M. Tour, ACS Nano **5**, 1535 (2011).
[7]R. H. Miwa, T. M. Schmidt, W. L. Scopel, and A. Fazzio, Appl. Phys. Lett. **99**, 163108 (2011).
[8]S. Adam, E. H. Hwang, V. M. Galitski, and S. Das Sarma, Proc. Natl. Acad. Sci. USA **104**, 18392 (2007).
[9]K. Zou, X. Hong, D. Keefer, and J. Zhu, Phys. Rev. Lett. **105**, 126601 (2010).
[10]S. M. Song and B. J. Cho, Nanotechnology **21**, 335706 (2010).
[11]Q. Chen, H. Huang, W. Chen, A. T. S. Wee, Y. P. Feng, J. W. Chai, Z. Zhang, J. S. Pan, and S. J. Wang, Appl. Phys. Lett. **96**, 072111 (2010).
[12]J. L. Moon, M. Antcliffe, H. C. Seo, D. Curtis, S. Lin, A. Schmitz, I. Milosavljevic, A. A. Kiselev, R. S. Ross, D. K. Kaskill *et al.*, Appl. Phys. Lett. **100**, 203512 (2012).
[13]B. Fallahazad, S. Kim, L. Colombo, and E. Tutuc, Appl. Phys. Lett. **97**, 123105 (2010).
[14]A. Pirkle, R. M. Wallace, and L. Colombo, Appl. Phys. Lett. **95**, 133106 (2009).
[15]G. Kresse and J. Furthmüller, Comput. Mater. Sci. **6**, 15 (1996).
[16]G. Kresse and J. Furthmüller, Phys. Rev. B **54**, 11169 (1996).
[17]D. Vanderbilt, Phys. Rev. B **41**, 7892 (1990).
[18]J. P. Perdew, K. Burke, and M. Ernzerhof, Phys. Rev. Lett. **77**, 3865 (1996).
[19]W. L. Scopel, A. J. R. da Silva, and A. Fazzio, Phys. Rev. B **77**, 172101 (2008).
[20]S. Grimme, J. Comput. Chem. **27**, 1787 (2006).
[21]K. Kamiya, N. Umezawa, and S. Okada, Phys. Rev. B **83**, 153413 (2011).
[22]S. P. Beckman, J. Han, and J. R. Chelikowsky, Phys. Rev. B **74**, 165314 (2006).
[23]N. T. Cuong, M. Otani, and S. Okada, Phys. Rev. Lett. **106**, 106801 (2011).
[24]The HfO_2 surface corrugations were inferred by the calculation of the root mean square deviation of vertical positions of the topmost O atoms, while for the adsorbed graphene sheet we considered the root mean square deviation of vertical positions of the graphene C atoms.
[25]H. Romero, N. Shen, P. Joshi, H. R. Gutierrez, S. A. Tadigadapa, J. O. Sofo, and P. C. Eklund, ACS Nano **2**, 2037 (2008).
[26]S. Guha and V. Narayanan, Phys. Rev. Lett. **98**, 196101 (2007).
[27]S. Walsh, L. Fang, J. K. Schaeffer, E. Weisbrod, and L. J. Brillson, Appl. Phys. Lett. **90**, 052901 (2007).
[28]C. G. Van de Walle and J. Neugebauer, J. Appl. Phys. **95**, 3851 (2004).
[29]Hafnium and oxygen chemical potentials, μ_{Hf} and μ_{O}, respectively, present an energy range, where the upper limit are given by $\mu_{[\mathrm{Hf}]}$ and $\mu_{[\mathrm{O}_2]}$, that is, the total energies of Hf bulk phase and isolated O_2 molecule. The lower limit for the oxygen chemical potential $\mu_{\mathrm{O}}^{\mathrm{min}}$ is determined by the enthalpy of formation of HfO_2 ($\Delta H_{[\mathrm{HfO}_2]}$), $\mu_{\mathrm{O}}^{\mathrm{min}} = \Delta H_{[\mathrm{HfO}_2]}/2 + \mu_{[\mathrm{O}_2]}$.
[30]G. L. Humphrey, J. Am. Chem. Soc. **75**, 2806 (1953).
[31]K. Xiong, J. Robertson, M. C. Gibson, and S. J. Clark, Appl. Phys. Lett. **87**, 183505 (2005).
[32]C. Stampfer, F. Molitor, D. Graf, K. Ensslin, A. Junger, C. Hierold, and L. Wirtz, Appl. Phys. Lett **91**, 241907 (2007).
[33]R. Bader, *Atoms in Molecules: A Quantum Theory* (Oxford University Press, New York, 1990).
[34]A. S. Foster, F. Lopez Gejo, A. L. Shluger, and R. M. Nieminen, Phys. Rev. B **65**, 174117 (2002).